Journal of Zhejiang University-SCIENCE A (Applied Physics & Engineering)
ISSN 1673-565X (Print); ISSN 1862-1775 (Online)
www.zju.edu.cn/jzus; www.springerlink.com
E-mail: jzus@zju.edu.cn

Numerical study on the aerodynamic performance and safe running of high-speed trains in sandstorms*

Hong-bing XIONG[1], Wen-guang YU[1], Da-wei CHEN[2], Xue-ming SHAO[†‡1]

([1]*Department of Mechanics, Zhejiang University, Hangzhou 310027, China*)

([2]*National Engineering Laboratory for System Integration of High-Speed Train (South), CSR Qingdao Sifang Co., Ltd., Qingdao 266111, China*)

[†]E-mail: mecsxm@zju.edu.cn

Received Sept 23, 2011; Revision accepted Sept 24, 2011; Crosschecked Sept 24, 2011

Abstract: The influence of sandstorms on train aerodynamic performance and safe running was studied in response to the frequent occurrence of sandstorm weather in north China. An Eulerian two-phase model in the computational fluid dynamic (CFD) software FLUENT, validated with published data, was used to solve the gas-solid multiphase flow of a sandstorm around a train. The train aerodynamic performance under different sandstorm levels and no sand conditions was then simulated. Results showed that in sandstorm weather, the drag, lift, side forces and overturning moment increase by variable degrees. Based on a numerical analysis of aerodynamic characteristics, an equation of train stability was also derived using the theory of moment balance from the view of dynamics. A recommended speed limit of a train under different sandstorm levels was calculated based on the stability analysis.

Key words: High-speed train, Sandstorm, Gas-solid multiphase, Eulerian two-phase model, Aerodynamic, Safety, Speed limit
doi:10.1631/jzus.A11GT005 **Document code:** A **CLC number:** O359; TD524

1 Introduction

China Railways has made a great leap forward during the last decade, and now being the largest exporter and licensor of high-speed railways in the world. The most significant progress has been made with regard to the rapid growth of railway construction and the innovation of the high-speed train. With train speed increasing, some extreme weather condition, for example, a crosswind or sandstorm, may severely limit the speed and affect the safe running of a railway train, especially in north China. Due to the dry climate and desertification in that region, severe winds and sandstorms occur all year round (Qiu, 2011; Zhang, 2011). In strong sandstorm weather, wind speed and sand concentration are high. The running of trains during such weather conditions may cause derailment, overturning or other serious train accidents. For example, many rollover accidents have occurred on the Lanzhou-Xinjiang Railway Line (Fig. 1). The north China has a dense railway network, so train safety in sandstorms is an important issue to study.

Many Chinese scholars have studied the effects of strong crosswinds on trains in recent years. Several wind tunnels have been constructed to carry out various experiments including studies of the aerodynamic performance of trains, tests of trains passing by each other and tests of stability in crosswinds (Tian and Liang, 1998; Tian and Lu, 1999; Gao *et al.*, 2007). Besides these experiments, numerical simulation provides another efficient tool to study these issues (Tian and He, 2001; Tian and Gao, 2003; Chen *et al.*, 2009). Similar research has also been carried out in some other countries with well-developed railways such as Japan, Germany, France and Sweden. These studies included train safety under crosswinds

‡ Corresponding author

* Project (No. 2009BAG12A01-C03) supported by the National Key Technology R&D Program of China

(Sanquer *et al.*, 2004; Baker, 2010), train slipstream effect, and drag reduction and aerodynamic performance (Watkinsa *et al.*, 1992). However, for trains under sandstorm conditions, less attention has been paid and their effects on the aerodynamic characteristics and train safety are unknown.

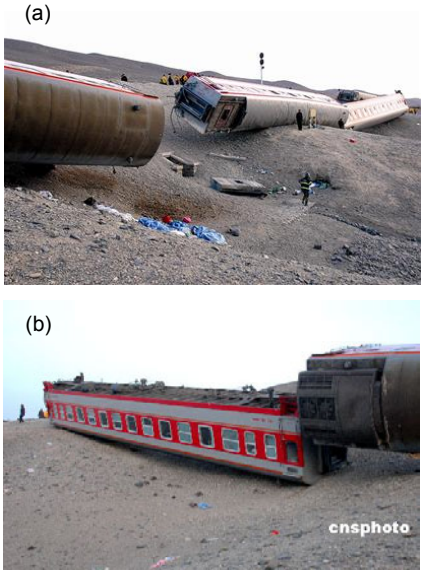

Fig. 1 Overturning accidents on Lanzhou-Xinjiang Railway Line on Feb. 28, 2007 (reported by China Daily)

A sandstorm is a typical two-phase flow problem with gas air and solid sand particles. Currently, this kind of flow is modeled mainly using two approaches: the Eulerian-Lagrangian (EL) and Eulerian-Eulerian (EE). In EL (Kuo *et al.*, 2002; Lun, 1984), the fluid is treated as a continuum phase by solving the Navier-Stokes equation, while the dispersed-phase is solved by tracking a large number of individual particles. Though providing more details of the particle phase, the EL approach is not suitable for large-scale engineering simulation with numerous dispersed particles, due to the limitations of finite memory capacity and CPU efficiency. The EE approach is more efficient and usually more complex (Ding, 1990; Gidaspow, 1994). In EE, each phase is treated as a continuous medium that may interpenetrate other phases, and is described by a set of equations with regard to momentum, continuity and energy. EE has been successfully applied to the simulation of pneumatic transport, fluidized beds, and other gas-solid multiphase flows with large numbers of particles in large equipment (van Wachem *et al.*, 1998; Zha, 2000). EE has also been used to simulate the influence of sandstorms on high-rise buildings (Wang and Wu, 2009). The train simulation in this study was complicated by the large computational domain and the large number of particles. Therefore, the EE approach was chosen instead of EL.

In this paper, the EE two-phase model is used to simulate the sandstorm flow around a train. Firstly, the numerical model is validated using published data. Then, the train aerodynamic performance under different sandstorm levels and no sand conditions is investigated. Finally, an equation of train stability is derived using the theory of moment balance from the view of dynamics, and a recommended speed limit for the train is calculated for different sandstorm levels.

2 Mathematical model and numerical simulation

2.1 Eulerian-Eulerian multiphase model

The continuity equation for the kth phase is

$$\frac{\partial}{\partial t}(f_k\rho_k)+\nabla(f_k\rho_k U_k)=0, \tag{1}$$

where the subscript k represents different phases: when k=g, it represents gas, when k=s, it represents the solid particle phase; f_k represents the volume fraction of the k phase. In current EE models, $f_k+f_s=1$. ρ_k represents the density of the k phase, ρ_g= 1.225kg/m^3, ρ_s=2500 kg/m^3; and U_k represents the velocity of the k phase.

The momentum equation of the gas phase is

$$\begin{aligned}&\frac{\partial}{\partial t}(f_g\rho_g U_g)+\nabla(f_g\rho_g U_g U_g)\\&\quad=-f_g\nabla p+\nabla\tau_g+f_g\rho_g g+K_{sg}(U_s-U_g),\end{aligned} \tag{2}$$

where p represents the pressure of the gas phase and solid phase. τ_g is the viscous shear tensor of gas. g is acceleration due to gravity, g=9.8 m/s^2, and K_{sg}=K_{gs} represents the gas-solid momentum exchange term.

The momentum equation of solid phase is

$$\begin{aligned}&\frac{\partial}{\partial t}(f_s\rho_s U_s)+\nabla(f_s\rho_s U_s U_s)\\&\quad=-f_s\nabla p-\nabla p_s+\nabla\tau_s+f_s\rho_s g+K_{gs}(U_g-U_s),\end{aligned} \tag{3}$$

where p_s is the pressure of solid: $p_s = \alpha_s \rho_s \theta_s + 2\rho_s(1+e_s)\alpha_s^2 g_0 \theta_s$, e_s=0.7 is the coefficient of restitution, and g_0 is the radical distribution function, which represents the probability of collision between sand. θ_s is the temperature of the sand and varies in direct ratio to the random kinetic energy of sand. The same model has been used in our group to study the train aerodynamic performance and safe operation under strong rainstorm condition (Shao *et al.*, 2011).

2.2 Computational simulation

The train in this study is a simplified model of the CRH2 (China Railway High-Speed 2), including three coaches: the head, middle and tail (Zhang, 2008). To fully develop the flow around the train and to ensure the accuracy of the results, a large semi-cylindrical numerical wind tunnel was established as the computational domain. The tunnel was 400 m wide in the horizontal direction, 600 m long in the axial direction and 200 m high in the vertical direction (Fig. 2a). The train had a length of 76.2 m, and was located on the centerline of the tunnel with an axial distance of 200 m from the train centroid to the tunnel inlet. In the preprocessing of mesh generation, a tetrahedral/hexahedral hybrid grid was adopted (Fig. 2b), and the number of grids was about 1.26 million.

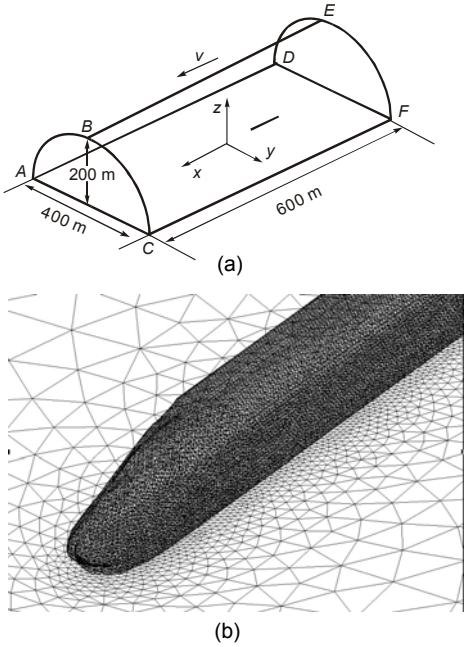

Fig. 2 Computional domain (a) and grid (b)

The velocity inlet and pressure outlet boundary conditions were adopted for both gas and solid phases. Owing to the small volume of the sand fraction, constant velocities of fluid and solid were specified equally with given phase fractions. For the gas phase, no slip wall boundary condition was adopted for the train walls. For the solid phase, a partial slip boundary condition was adopted with a specified specularity coefficient of 0.1.

2.3 Validation of the numerical model

2.3.1 Verification of Eulerian two-phase model

To verify the accuracy of the Eulerian two-phase model in the external flow, we first used an Eulerian two-phase mode to simulate the aerodynamic characteristics of the airfoil NACA64-210 in a rain environment, and compared the numerical results with published experimental data (Bezos *et al.* 1992). The drag force (C_d) at different angle of attack (α_a) was illustrated in Figs. 3 and 4 for experiments and simulations, respectively. Our simulation results agreed reasonably well with the experimental data.

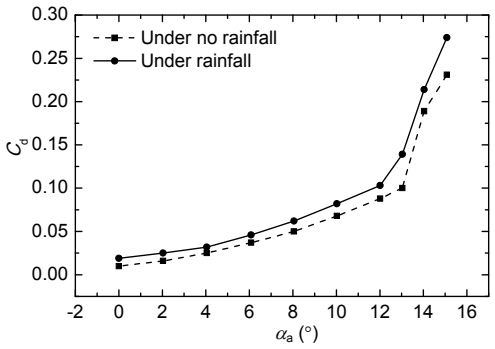

Fig. 3 Experimental results for the drag coefficient of an airfoil under no rain and rain environments

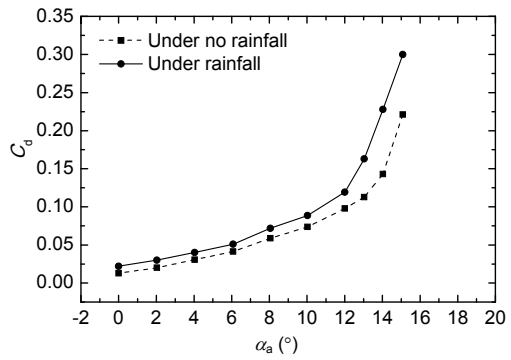

Fig. 4 Numerical results for the drag coefficient of an airfoil under no rain and rain environments

2.3.2 Verification of the train model

To validate the train model of numerical simulation, grid dependency was conducted with three sizes of grid generation: 1.95 million, 1.26 million and 0.54 million, respectively. Comparing the train aerodynamic performance, we found that the difference between the results from 1.26 million grids and from 1.95 million grids was only about 2%, while the result from 0.54 million grids was very different from those two cases. Therefore, considering the accuracy and efficiency of calculation, 1.26 million grids were adopted.

In this study, we reduced the geometrical complexity and used a simplified train model without the bogies, pantograph and windshield, for computational efficiency. In our previous study, the aerodynamic characteristics of the complete train model were calculated and gave a drag coefficient of C_x=0.385, compared with the experimental data result of C_x=0.393 (Zhang and Xiong, 2011). The good correspondence of these results demonstrates that our numerical model for the CRH2 train is reliable.

3 Results and discussion

Sandstorm weather is divided into six levels according to its intensity. The typical values of sand concentration and wind velocity for different sandstorm levels are shown in Table 1.

The aim of this study was to simulate the aerodynamic performance of the train in different wind speeds and different sandstorm levels. Detailed cases were as follows:

Under sand conditions, the speed of the train is V_t=300 km/h, and the sandstorm levels are floating dust, blowing dust, weak sandstorm, medium sandstorm, strong sandstorm, and particularly strong sandstorm (Table 1).

Under no sand conditions, the speed of the train is V_t=300 km/h, and the wind speeds (V) are 5, 10, 15, 20, 25, and 30 m/s , respectively, corresponding to the sandstorm levels.

Among the aerodynamic forces, the drag force F_x, lift force F_y, side force F_z, and overturning moment M_x play vital roles in train aerodynamics and safe running in sandstorm conditions. Therefore, we will first focus on the influence of sand on these forces.

3.1 Influence of sand on the drag force

The drag force of the train under sand conditions and no sand conditions are shown in Fig. 5. F_{x0} and F_{x1} represent the drag under no sand conditions and sand conditions, respectively. From the curve F_{x0}, we find that the drag increases when there is a crosswind. Note that the drag decreases at a relatively large wind speed, though drag force increases with the wind speed. The reason is that the drag is based on the sum of train and wind velocity. The trend curve of F_{x1} is similar to that of F_{x0}, but the values of F_{x1} are much bigger than those of F_{x0}, due to the effects of the sand. So we can conclude that the sand increases the drag force of the train, and the higher the level of sandstorm, the higher the increase in drag force.

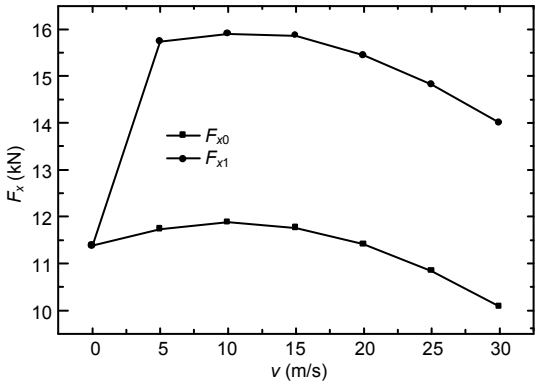

Fig. 5 Drag force of the train under no sand and sand environments

Table 1 Wind speeds and sand concentrations for different sandstorm levels

Sandstorm	TSP* (mg/m^3)	Volume fraction of sand	Wind speed (m/s)
Floating dust	0.4	1.6×10^{-10}	5
Blowing dust	1.2	4.8×10^{-10}	10
Weak sandstorm	6	2.4×10^{-9}	15
Medium sandstorm	30	1.2×10^{-8}	20
Strong sandstorm	90	3.6×10^{-8}	25
Particularly strong sandstorm	270	1.08×10^{-7}	30

* TSP: total suspended particulate

3.2 Influence of sand on the lift force

The lift force of a train is an important factor that affects its safety and comfort. A large lift force will bring instability and discomfort to the passengers, and may even cause the train to overturn. If the lift force is positive with an upward direction, the adhesive force between the wheels and the railway lines reduces so that the possibility of derailment increases. A negative lift force with a small value is favorable as it will increase the contact force between the wheels and the railway lines.

The lift forces of the train under sand conditions (F_{z1}) and no sand conditions (F_{z0}) are shown in Fig. 6. The trend of these two curves is the same: both F_{z1} and F_{z0} grow with the wind speed corresponding to sandstorm level. But the lift force under sand is bigger than that under no sand, and the difference grows with the sandstorm level. The force under particularly strong sandstorm conditions is about 50% larger than that under no sand conditions. So the sand increases the value of the lift force significantly: the stronger is the sandstorm, the higher the lift force, and the lower the train's stability.

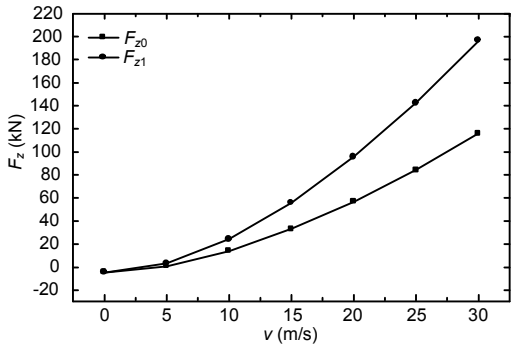

Fig. 6 Lift forces of the train under no sand and sand environments

3.3 Influence of sand on the side force

Owing to the asymmetric structure of flow around the train, the pressure distribution on the surface of the train is asymmetric, which leads to a differential pressure side force. Viscous shear stress acts on the surface that forms the side friction force. The sum of the differential pressure side force and the side friction force is the total side force F_y (Fig. 7).

As predicted, the side force increases with the speed of the crosswind. The force under sand conditions (F_{y1}) is larger than that under no sand (F_{y0}). The difference between them grows with the level of sandstorm. The side force under particularly strong sandstorm conditions increases by 33.5%. The sand increases the side force and may reduce the train's stability.

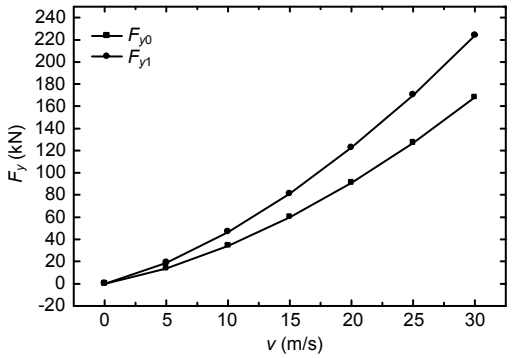

Fig. 7 Side forces of the train under no sand and sand environments

3.4 Influence of sand on the overturning moment

The overturning moment, M_x, is the moment generated by the aerodynamics of the train around the vertical axis (x-axis) and tending to overturn the train (Fig. 8). The overturning moment significantly affects the stability of the train. M_x increases dramatically with crosswind, and also increases with wind speed. The value of overturning moment under sand conditions (M_{x1}) is larger than that under no sand conditions (M_{x0}). The difference between M_{x0} and M_{x1} increases with the growing level of the sandstorm. So the sand reduces the stability of trains in a crosswind.

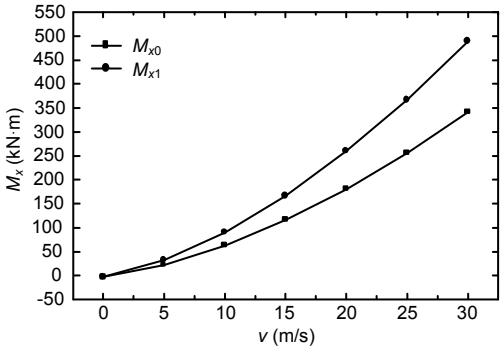

Fig. 8 Overturning moments of the train under no sand and sand environments

3.5 Influence of sand on the train's safety and recommended speed limit under crosswind

The stability of a train against overturning or derailment is usually used to evaluate safety performance when a train runs on straight or curved rails in a crosswind. When running on curved rails, the outer rail is higher than the inner rail and an unbalanced centrifugal force will be generated. The centrifugal force combined with the side force generated by a crosswind, and the inertia force of transversal vibration increase the possibility that the train will turn over. There are three ways in which a train may turn over: (1) Running on straight rails, the train will turn over in the direction of the crosswind; (2) Running on curved rails, the train will turn over in the direction from the inside rail to the outside rail; (3) Running on curved rails, the train will turn over in the direction from the outside rail to the inside rail.

The running stability of a train depends on several factors including its shape, size, and mass, the height of its center of gravity, and its running speed. The relationship between the running speed limit and the crosswind speed can be derived from the dynamic torque balance principle. The method and formulas have been studied (Gao and Tian, 2004; Tian, 2007). This method is used in this study to calculate the speed limit of a train under different speeds of crosswind and sand conditions. The influence of sand on the speed limit was then analyzed by comparing the results with those obtained under no sand conditions. The procedure to derive the relationship between the speed limit and wind speed is as follows.

Firstly, the aerodynamic performance, under sand and no sand conditions, at different yaw angles α were simulated in the CFD software FLUENT. The yaw angle, defined as the angle between the train velocity vector and the resultant velocity vector, varied from 0° to 180°. In this study, we assumed that the direction of the crosswind was perpendicular to the velocity of the train. The three aerodynamic coefficients C_y, C_z, and C_{mx} were calculated. These coefficients are defined as follows:

$$C_i=\frac{F_i}{\frac{1}{2}\rho V_{TW}^2 S},\quad C_{mi}=\frac{M_i}{\frac{1}{2}\rho V_{TW}^2 SL}, \tag{4}$$

where $i=x, y, z$ for the force and moment components F_i and M_i in different direction, ρ=1.225 kg/m^3, S=268.34 m^2, L=76.2 m, and V_{TW} represents the resultant velocity of train and wind speed. The curves of C_y–α, C_z–α, and C_{mx}–α under two weather conditions were plotted, respectively (Fig. 9), and the fitting results of the relationships between the aerodynamic coefficients and yaw angle α were:

Under no sand conditions:

$$C_{mx}=-2.72777\times10^{-9}\alpha^3-4.9575\times10^{-5}\alpha^2+9.005\times10^{-3}\alpha,$$
$$C_y=-2.8445\times10^{-9}\alpha^3-8.2909\times10^{-5}\alpha^2+1.501\times10^{-2}\alpha,$$
$$C_z=-2.8308\times10^{-9}\alpha^3-9.5106\times10^{-5}\alpha^2+1.721\times10^{-2}\alpha.$$

Under sand conditions:

$$C_{mx}=-2.7789\times10^{-9}\alpha^3-6.4072\times10^{-5}\alpha^2+1.1615\times10^{-2}\alpha,$$
$$C_y=-2.918\times10^{-9}\alpha^3-1.07220\times10^{-4}\alpha^2+1.9386\times10^{-2}\alpha,$$
$$C_z=-3.1229\times10^{-9}\alpha^3-1.229\times10^{-4}\alpha^2+2.2213\times10^{-2}\alpha.$$

Finally, taking the results above to the moment balance formulas, the speed limits of the train running on straight or curved rails under different crosswind speeds and sand conditions were calculated (Tables 2 and 3).

Form Tables 2 and 3, we find that, at the same yaw angle, the speed limit of train is the highest on curved rails when the train is to turn over from the outside to the inside rails; the limit speed is the lowest when the train is to turn over from the inside to the outside rails; the limit speed on straight rails is intermediate. At the same yaw angle, the limit speed of the train under sand conditions is smaller than that under no sand conditions, decreasing about 10%–15%. In other words, a sandstorm reduces the safe speed limit of trains at a given crosswind speed. The safe running performance is reduced in sandstorm weather.

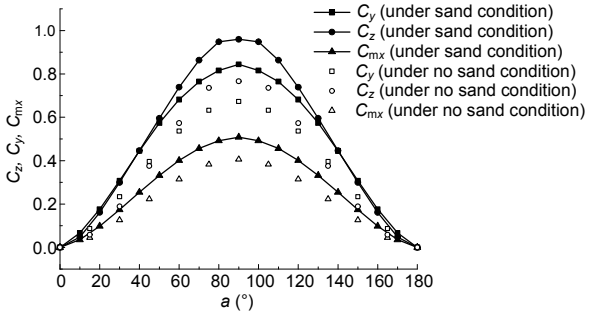

Fig. 9 Aerodynamic coefficients under no sand and sand conditions

Table 2 Relationship between the train speed limit and crosswind speed under no sand conditions

α (°)	Straight line		Turning form outside to inside		Turning form inside to outside	
	V_w (m/s)	V_t (m/s)	V_w (m/s)	V_t (m/s)	V_w (m/s)	V_t (m/s)
15	17.799	66.461	20.799	77.666	15.718	58.691
30	25.494	44.184	27.490	47.643	23.797	41.243
45	31.022	31.047	32.689	32.716	29.513	29.536
60	34.892	20.170	36.406	21.045	33.485	19.356
75	37.205	9.996	38.644	10.382	35.853	9.632
90	37.979	0.030	39.389	0.0314	36.640	0.029

V_t: limit speed of train; V_w: limit speed of wind

Table 3 Relationship between the train speed limit and crosswind speed under sand conditions

α (°)	Straight line		Turning form outside to inside		Turning form inside to outside	
	V_w (m/s)	V_t (m/s)	V_w (m/s)	V_t (m/s)	V_w (m/s)	V_t (m/s)
15	15.669	58.507	17.561	65.573	14.215	53.081
30	22.444	38.898	23.721	41.112	21.297	36.910
45	27.312	27.334	28.375	28.398	26.312	26.333
60	30.722	17.759	31.678	18.312	29.801	17.227
75	32.764	8.802	33.667	9.045	31.886	8.567
90	33.442	0.027	34.330	0.027	32.577	0.0259

V_t: limit speed of train; V_w: limit speed of wind

4 Conclusions

In this paper, an EE multiphase model was used to study the performance of a train running under different levels of sandstorm weather, and the results were compared with that from no sand conditions. The influence of sand on aerodynamic performance was analyzed parametrically. Results indicate that the drag, lift, side forces and overturning moment increase in sandstorm weather, and the sand effect increases with the level of sandstorm. Finally, according to the quasi-static analysis method of moment balance, the safe running speed limit of the train was calculated under sandstorm conditions and no sand conditions. The results indicated that a sandstorm reduces the speed limit of the train.

References

Baker, C.J., 2010. The simulation of unsteady aerodynamic cross wind forces on trains. *Journal of Wind Engineering and Industrial Aerodynamics*, **98**(2):88-99.

Bezos, G.M., Dunham, R.E., Gentry, G.L., Melson, W.E., 1992. Wind Tunnel Aerodynamic Characteristics of a Transport-Type Airfoil in a Simulated Heavy Rain. Environment Technical Report, NASA Technical Paper, **3184**:66-87.

Chen, R.L., Zeng, Q.Y., Zhong, X.G., Xiang, J., Guo, X.G., Zhao, G., 2009. Numerical study on the restriction speed of train passing curved rail in cross wind. *Journal of Science in China Series*, **52**(7):2037-2047. [doi:10.1007/s11431-009-0202-5]

Ding, J.M., Gidaspow, D., 1990. A bubbling fluidization model using kinetic theory of granular flow. *AIChE Journal*, **36**(4):523-538.

Gao, G.J., Tian, H.Q., 2004. Effect of strong crosswind on the stability of trains running on the Lanzhou-Xinjiang railway line. *Journal of the China Railway Society*, **26**(4):36-41.

Gao, G.J., Tian, H.Q., Miao, X.J., 2007. Research on the stability of box-car on Qinghai-Tibet Railway Line under strong cross wind. *Science Paper Online*, **2**(9):684-987.

Gidaspow, D., 1994. Multiphase Flow and Fluidization. Academic Press, Boston.

Kuo, H.P., Knight, P.C., Tsuji, Y., 2002. The influence of DEM simulation parameters on the particle behaviour in a V-mixer. *Chemical Engineering Science*, **57**:3621-3638.

Lun, C.K.K., Savage, S.B., Jeffrey, D.J., Chepurniy, N., 1984. Kinetic theories for granular flow: inelastic particles in Couette flow and slightly inelastic particles in a general flowfield. *Journal of Fluid Mechanics*, **140**:223-256.

Qiu, X.F., Zeng, Y., Miu, Q.L., 2011. Temporal-spatial distribution as well as tracks and source areas of sand-dust storms in China. *Actageographica Sinica*, **56**(3):318-319.

Sanquer, S.S., Barréa, C., de Virel, M.D., Cléon, L.M., 2004. Effect of cross winds on high-speed trains: development of a new experimental methodology. *Journal of Wind Engineering and Industrial Aerodynamics*, **92**(7-8): 535-545.

Shao, X.M., Wan, J., Chen, D.W., Xiong, H.B., 2011. Aerodynamic modeling and stability analysis of a high-speed train under strong rain and crosswind conditions. *Journal of Zhejiang University SCIENCE-A (Applied Physics and Engineering)*, **12**(12):964-970. [doi:10.1631/jzus.A11GT001]

Tian, H.Q., 2007. Train Aerodynamics. China Railway Publishing House, Beijing, China.

Tian, H.Q., Liang, X.F., 1998. Test research on crossing air pressure pulse of quasi-high-speed train. *Journal of the China Railway Society*, **4**(7):1-8.

Tian, H.Q., Lu, Z.Z., 1999. Air tunnel test and research on the control car in 200 km/h electrical passenger train unit. *Journal of the China Railway Society*, **12**(7):15-18.

Tian, H.Q., He, D.X., 2001. 3-D numerical calculation of the air pressure pulse from two trains passing by each other. *Journal of the China Railway Society*, **23**(3):18-22.

Tian, H.Q., Gao, G.J., 2003. The analysis and evaluation on the aerodynamic behavior of 270 km/h high-speed train. *Journal of the China Railway Society*, **24**(2):14-18.

van Wachem, B.G.M., Schouten, J.C., Krishna, R., van den Bleek, C.M., 1998. Eulerian simulations of bubbling behaviour in gas-solid fluidised beds. *Computers and Chemical Engineering*, **22**(Supp.):299-307.

Wang, W., Fang, Z.Y., 2004. Review of duststorm weather and research progress. *Journal of Applied Meteorological Science*, **15**(3):366-380.

Wang, S.T., Wu, S.Z., 2009. Numerical Simulation of Drifting Sand Flow Field on High-Rise Buildings. MS Thesis, Lanzhou University, China (in Chinese).

Watkinsa, S., Saundersa, J.W., Kumara, H., 1992. Aerodynamic drag reduction of goods trains. *Journal of Wind Engineering and Industrial Aerodynamics*, **40**(2): 147-178.

Zha, X.D., Fan, J.R., Sun, P., Cen, K.F., 2000. Numerical simulation on dense gas-particle riser flow. *Journal of Zhejiang University SCIENCE*, **1**(1):29-38.

Zhang, S.G., 2008. The CRH-2 High-Speed Train. China Railway Publishing House, Beijing, China.

Zhang, M., Xiong, H.B., 2011. Effects of different components on the aerodynamics of high-speed train. *Journal of Manufacturing Automation*, **33**(4):202-205.

Zhang, X.L., Zhang, Y.F., 2011. Causes of sand-dust storm in northern China in recent years and its control. *Journal of Catastrophology*, **16**(3):70-76.